From siphonophores to deep scattering layers: uncertainty ranges for the estimation of global mesopelagic fish biomass

Roland Proud[1]*, Nils Olav Handegard[2], Rudy J. Kloser[3], Martin J. Cox[4], and Andrew S. Brierley[1]

[1]Pelagic Ecology Research Group, Gatty Marine Laboratory, Scottish Oceans Institute, University of St Andrews, St Andrews, Fife KY16 8LB, UK
[2]Institute of Marine Research, PO Box 1870, Nordnes, 5817 Bergen, Norway
[3]CSIRO Oceans and Atmosphere Flagship, GPO Box 1538, Hobart, TAS 7001, Australia
[4]Australian Antarctic Division, 203 Channel Highway, Kingston, Tasmania, 7050 Australia

*Corresponding author: tel: +44 (0)1334 46 3401; e-mail: rp43@st-andrews.ac.uk.

The mesopelagic community is important for downward oceanic carbon transportation and is a potential food source for humans. Estimates of global mesopelagic fish biomass vary substantially (between 1 and 20 Gt). Here, we develop a global mesopelagic fish biomass model using daytime 38 kHz acoustic backscatter from deep scattering layers. Model backscatter arises predominantly from fish and siphonophores but the relative proportions of siphonophores and fish, and several of the parameters in the model, are uncertain. We use simulations to estimate biomass and the variance of biomass determined across three different scenarios; S1, where all fish have gas-filled swimbladders, and S2 and S3, where a proportion of fish do not. Our estimates of biomass ranged from 1.8 to 16 Gt (25–75% quartile ranges), and median values of S1 to S3 were 3.8, 4.6, and 8.3 Gt, respectively. A sensitivity analysis shows that for any given quantity of fish backscatter, the fish swimbladder volume, its size distribution and its aspect ratio are the parameters that cause most variation (i.e. lead to greatest uncertainty) in the biomass estimate. Determination of these parameters should be prioritized in future studies, as should determining the proportion of backscatter due to siphonophores.

Keywords: acoustics, DSLs, myctophids, pneumatophore, resonance, scattering models, swimbladder.

Introduction

In this article, we consider, from the standpoint of available acoustic survey data, what the global biomass of mesopelagic fish (fish in the 200–1000 m depth range, including myctophids or "lantern fish") might be.

The importance of the mesopelagic community

The mesopelagic community plays an important role in global biogeochemical cycling and the biological carbon pump, and is attracting increasing attention from commercial fishers (St John et al., 2016). Biogeochemical and ecosystem models which simulate the biological carbon pump require validation of the mesopelagic component to provide confidence in their predictions of vertical carbon flux, which itself feeds into climate/Earth-system models (Giering et al., 2014). To cast light on the "dark hole in our understanding" of the mesopelagic (St John et al., 2016), to progress towards ecosystem-based management in advance of developing fisheries, and to make headway on conservation of water-column habitat in areas beyond national jurisdiction (Roberts et al., 2017), a robust estimate of mesopelagic fish biomass is required.

A substantial amount of mesopelagic biomass in the 1 mm+ size fraction is contained, during the day, within deep scattering layers (DSLs), primarily made up of fish, zooplankton, squid, and jellyfish. DSLs are detected using echosounders, which emit sound waves and record backscatter (see Chu, 2011, for a review). Echosounder

observations (summarized pictorially as echograms) can be analysed and biological features such as layers, schools, and swarms can be identified and quantified (Holliday, 1972; Coetzee, 2000; Cox et al., 2011; Proud et al., 2015). DSL depth varies globally between ~200 and 1000 m and is driven, at least in part, by environmental conditions, e.g. light intensity, oxygen concentration, temperature, and mixing (Bianchi et al., 2013; Klevjer et al., 2016; Aksnes et al., 2017; Proud et al., 2017). There is often more than one single scattering layer (e.g. Andreeva et al., 2000). DSL backscattering intensity (a proxy for biomass) also varies globally and is correlated with primary production (PP) at the surface and temperature at DSL depth (Netburn and Koslow, 2015; Proud et al., 2017). Typically, DSL backscatter reduces during the night, as a proportion of the community migrates to the surface to feed (Brierley, 2014).

Present estimates of mesopelagic fish biomass

It has been estimated recently that the global biomass of mesopelagic fish could be around 11–15 gigatonnes (Gt) (Irigoien et al., 2014). That estimate arises from analysis of an acoustic survey (38 kHz) transect run west to east around the world through the mid latitudes (the *Malaspina* 2010 Circumnavigation Expedition). Under that analysis, the acoustic backscatter is attributed 100% to fish and the resulting biomass estimate is ~11–15 times higher than an historic estimate of 1 Gt based on net sampling (Gjøsaeter and Kawaguchi, 1980). Although it is recognized that trawl avoidance by mesopelagic fish may lead to a large underestimation of their biomass by net sampling (Kaartvedt et al., 2012), acoustic energy is not necessarily directly proportional to fish biomass and the acoustic energy is not only from fish and so the disagreement between "historic" and "new" estimates could be due to inaccuracy in both assumptions rather than just to a failing of one.

Proud et al. (2017) compiled a quasi-global database of daytime 38 kHz mesopelagic backscattering intensity, and used it to define a mesopelagic biogeography. The biogeography was compiled from completely different acoustic data to the *Malaspina* study, with a much wider geographic extent, and was based on characteristics of objectively identified DSLs. Total backscatter arising from DSLs in the mesopelagic zone (200–1000 m) was predicted to be $6.02 \pm 1.4 \times 10^9$ m^2 (mean area-backscattering coefficient multiplied by surface area). In previous work, we scaled this prediction to global fish biomass (70° N and 70° S), estimating a value of 9 Gt (Proud, 2016). Irigoien et al. (2014) suggest that their estimate (11–15 Gt for the geographic region between latitudes 40° N and 40° S) could be ~30% higher (i.e. 14.3–19.5 Gt) if expanded to the area between 70° N and 70° S, which is similar to the extent of the Proud et al. (2017) biogeography. That scaled estimate is startlingly high, and begs the question "can it even be sustained given known PP?" Back-of-the envelope trophic calculations reveal that "yes, it can": for a given value of PP, temperature and trophic efficiency (TE), the biomass of mesopelagic fish (trophic level = 3.2, www.fishbase.org) can be predicted (Gascuel et al., 2008). For TE values of 5, 10, and 20%, a global mean temperature at the depth of the DSL of 7.2°C and average open-ocean PP of 0.312 g C d^{-1} (Proud et al., 2017), global mesopelagic fish biomasses are predicted to be c. 0.73, 3.4, and 15.5 Gt, respectively. Recent high mesopelagic estimates are therefore at least energetically possible if TEs to mesopelagic fish are of the order of 20% (Davison et al., 2013; Heymans et al., 2014; Rosenberg et al., 2014; Jennings and Collingridge, 2015). However, a recent food-web model (Anderson et al., 2018) and a macroecological model (Jennings and Collingridge, 2015), predict global mesopelagic fish biomass of 2.4 and <1.4 Gt (median biomass for all consumers including mesopelagic fish), respectively: these are closer to the historic mesopelagic fish biomass estimate of 1 Gt (Gjøsaeter and Kawaguchi, 1980).

Gas-bladdered mesopelagic siphonophores and fish

The mesopelagic zone is occupied by a range of taxa, including crustacean and gelatinous zooplankton and cephalopods. Some of these can be numerically very abundant (e.g. copepods) and some have a high acoustic target strength (TS). Gas-bearing siphonophores (Physonects and Cystonects) and teleost fish, with gas-filled swimbladders are strong acoustic targets (Barham, 1963, 1966; Warren, 2001; Scoulding et al., 2015) and resonant at depth at 38 kHz (Kloser et al., 2016). To estimate plausible ranges of mesopelagic fish biomass with acoustic data the effect of resonant scatter from siphonophores with gas-filled pneumatophores (gas bladders) and fish with gas-filled swimbladders (gas bladders) needs to be considered (Davison et al., 2015).

The TS from individual gas bladders (gas-filled organs of fish and siphonophores), produces >95% of the organism's total TS (Foote, 1987) and is often used to approximate the TS of a gas-bladdered fish or siphonophore (Warren, 2001; Scoulding et al., 2015). Gas bladder TS can be predicted using acoustic scattering models, typically assuming that the shape of the gas bladder can be approximated by a prolate spheroid (Scoulding et al., 2015). Modelled gas bladder TS increases linearly with size in the Rayleigh zone and plateaus as the size of the gas bladder approaches a value of $\lambda/2\pi$ in the geometric zone (Figure 1), where λ is the wavelength of the incident sound wave. In the resonant region (Figure 1), the gas bladder vibrates in sympathy with the acoustic wave and re-radiates more energy than predicted by commonly used log-linear TS-to-length relationships (e.g. Foote, 1987). The degree of the re-radiation is dependent somewhat on the tension of the gas bladder wall and the tissue viscosity (Love, 1978; Baik, 2013; Scoulding et al., 2015). In this study, acoustic data were available at the commonly used fisheries acoustic frequency of 38 kHz. The wavelength at 38 kHz in seawater is ~3.9 cm, and 38 kHz sound scattering by a mesopelagic fish or siphonophore at 500 m, with an *in situ* gas bladder ~1 mm in length, falls well within the resonant region. Resonant scattering will be provoked routinely in surveys at 38 kHz of mesopelagic fish and siphonophores when the equivalent spherical radius (the radius of a sphere equal in volume to the prolate spheroid) of the gas bladder is within ~0.4–1 mm (Davison et al., 2015; Kloser et al., 2016). Resonant scattering need not be confined just to "small" fish or siphonophores as the investment of fat in the swimbladders of older and larger fish (Neighbors and Nafpaktitis, 1982) may result in swimbladders of larger fish actually containing *smaller* volumes of gas than smaller fish; a reduction in body density with length may also contribute to this effect. Furthermore, compression of the gas bladders of downward-migrating fish, according to Boyle's Law, may result in the gas bladder volume being substantially smaller than would be suggested by fish length alone, and so diel variability in scattering type/intensity may occur. The issue of mesopelagic fish TS is clearly vexed.

Approach

We take the approach here of attempting to attribute received echo energy in plausible proportions to fish and other potential sound-scatterers, and to scale the likely echo energy from fish to
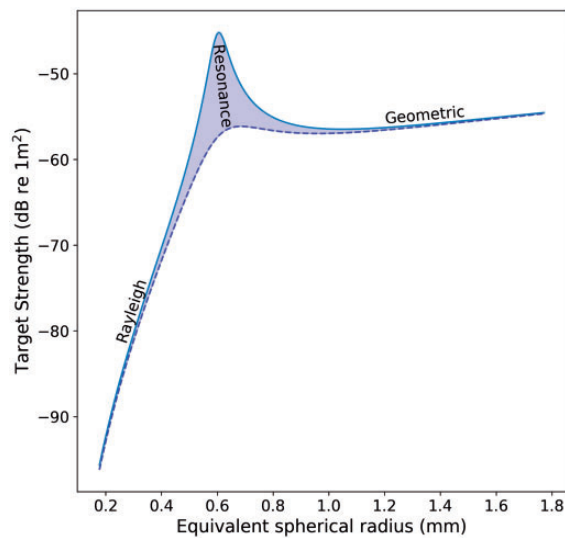
Figure 1. Predicted 38 kHz target strength (TS) of a gas bladder (gas-filled organs of fish and siphonophores) at 500 m over a range of sizes. The gas bladder was modelled as a prolate spheroid using a resonance acoustic scattering model (Scoulding *et al.*, 2015) and the equivalent spherical radius (a_{esr}) was calculated using $a_{esr} = (ab^2)^{1/3}$ where a and b are the semi-major and semi-minor axes of the prolate spheroid, respectively. Rayleigh and geometric scattering zones are indicated along with consequences to TS of resonance.

biomass in a manner that takes in to account non-linearity due to resonant scattering (Love, 1978). We do not seek formally to solve the "inverse" problem (Holliday *et al.*, 1989), rather to determine a realistically bounded indication of the possible ranges of global mesopelagic fish biomass. This approach is necessary because collectively science does not yet have, and indeed is not likely to have anytime soon, detailed information on the abundance and size of the community of organisms inhabiting the mesopelagic realm globally. That community is made up of a diverse range of taxa spanning a size range of several orders of magnitude, and no single sampling approach will yield an unbiased view. Net sampling, for example, delivers only slow-moving and physically robust organisms because the better swimmers (which tend to be larger) can evade nets, and fragile, gelatinous organisms are mangled by them (Pakhomov and Yamamura, 2010).

Objectives

The objective of this article is to estimate the likely range of global mesopelagic fish biomass and the drivers of uncertainty. Our method was as follows: (i) define a generalized acoustic biomass model, (ii) obtain a global mean value of mesopelagic backscatter from the literature (Proud *et al.*, 2017), (iii) with reference to acoustic scattering models, review the dominant sources of backscatter found within the mesopelagic zone, (iv) define mesopelagic fish biomass model and identify unknown parameters and possible confounding animal behaviours, (v) define plausible statistical distributions to capture the full range of uncertainty in the unknown parameters and develop scenarios to simulate a range of animal behaviours, (vi) quantify uncertainty across all scenarios

of mesopelagic fish biomass estimates, and (vii) run a global sensitivity analysis to quantify the contribution of each parameter to overall uncertainty in the mesopelagic fish biomass model.

Methods

The method presented here follows a generalized approach. We first define general equations used for the conversion of acoustic backscattering intensity to biomass (see also Equation 1 in Kloser *et al.*, 2009 and Equation 9.11 in Simmonds and MacLennan, 2005), and then parameterize them for estimation of mesopelagic fish biomass.

For a given aggregation of organisms, comprising G groups (e.g. taxonomic, functional, or anatomical), each made up of M_g members, over a common area A, the mean area-backscattering coefficient for all groups, s_a (m^2 m^{-2}), is given by

$$s_a = \frac{1}{A} \sum_{g=1}^{G} \sum_{m=1}^{M_g} \sigma_{bs_{g,m}}, \qquad (1)$$

where g is the group index, m is the group member index and $\sigma_{bs_{g,m}}$ (m^2) is the backscattering cross-section for member m of group g. Group biomass, B_g (kg), is then calculated by

$$B_g = A \frac{p_g s_a}{\overline{\sigma_{bs_g}}} \overline{W_g}, \qquad (2)$$

where $\overline{W_g}$ (kg) and $\overline{\sigma_{bs_g}}$ are the mean member weight and mean area-backscattering coefficient of group g and p_g, the proportion of s_a that is produced by group g, is given by

$$p_g = \frac{n_g \overline{\sigma_{bs_g}}}{\sum\limits_{g=1}^{G} n_g \overline{\sigma_{bs_g}}}, \qquad (3)$$

where n_g is the relative proportion by number of the aggregation represented by group g.

To estimate B_g, the following steps are taken: (i) define the group of interest (g), establish the region and depth range z_1 to z_2 (volume) which contains the group of interest, and define all other known scattering groups found within the volume; (ii) predict or measure s_a over the volume for a given incident frequency; (iii) define acoustic scattering models to predict $\overline{\sigma_{bs_g}}$ of each group; (iv) determine which groups contribute substantially to s_a and estimate p_g; (v) solve (2) for the group of interest, and identify unknown parameters and animal behaviours; (vi) define distributions for unknown parameters and scenarios for unknown animal behaviours; (vii) estimate uncertainty in B_g over the parameter space for each scenario; and (viii) determine the sensitivity of B_g to input parameters.

The remainder of the method follows this procedure for the case of the putative global population of mesopelagic fish.

Model definitions and global mesopelagic area-backscattering coefficient

In this study, we define our target group as fish in mesopelagic (200–1000 m) DSLs (Figure 2) during the daytime in the open ocean (seabed depth > 1000 m). Globally, there are c. 900 species of mesopelagic fish and the most abundant and diverse family group is Myctophidae (lanternfish) with c. 250 species (Bone *et al.*, 1995); other fish families which include large
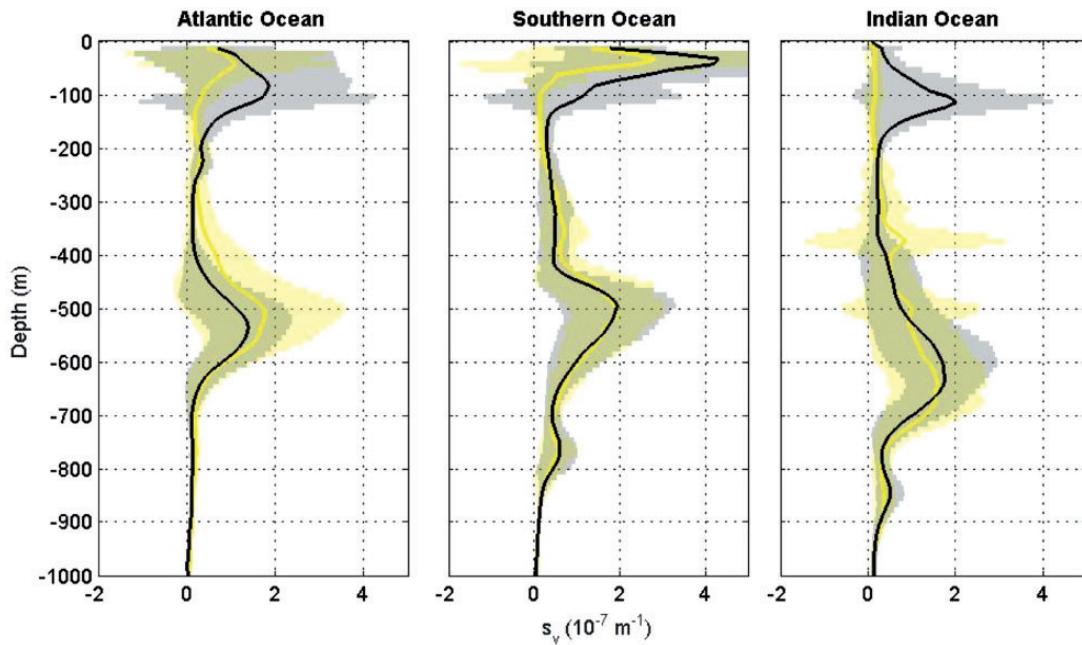
Figure 2. DSL day–night variability in three oceans. Mean linear volume backscattering coefficient (s_v, m^{-1}) in 10 m depth bins to 1000 m for day (yellow) and black (night) for 38 kHz acoustic survey data (source: www.imos.org.au). Shading represents the standard deviation of the s_v values. Dusk and dawn defined as 1 h prior to and after sunset and sunrise, respectively.

numbers of mesopelagic fish are Gonostomatidae (bristle-mouths), Phosichthyidae (lightfishes), and Sternoptychidae (e.g. marine hatchetfishes) (Bone *et al.*, 1995). The global open ocean has, following Proud *et al.* (2017), a total surface area, *A*, of 3.11×10^{14} m^2 and total global daytime 38 kHz mesopelagic backscatter of $6.02 \pm 1.4 \times 10^9$ m^2; at 38 kHz, the signal-to-noise ratio is such that the observable range is at least 1000 m. The global s_a value, determined by dividing the total mesopelagic backscatter by *A*, is $1.94 \pm 0.44 \times 10^{-5}$ m^2 m^{-2}. We contend that the following taxonomically based scattering groups make possible substantial contributions to mesopelagic s_a: copepods; euphausiids; squid; jellyfish; and siphonophores (Physonects and Cystonects, referred to collectively as just siphonophores from here on for simplicity).

Acoustic scattering models

The scattering groups defined here fall into two categories, gas-bearing organisms (mesopelagic fish and siphonophores) and weakly scattering fluid-filled organisms (copepods, euphausiids, squid, and jellyfish). The σ_{bs} of the fluid-filled group was predicted using the distorted-wave-born approximation (DWBA) model (Chu *et al.*, 1993) using parameters from Lavery *et al.* (2007).

The gas-filled swimbladders of fish (gas bladders) and gas-filled pneumatophores of siphonophores (gas bladders) produce >95% of the organisms' backscatter at 38 kHz (Foote, 1980). This figure is likely to be closer to 99% for mesopelagic fish: Foote (1980) refers to much larger and denser epipelagic fish for which backscatter from body tissue makes up a larger proportion of the total. The σ_{bs} of the gas bladders of fish and siphonophores can be predicted using the resonance model of Love

(1978), including adaptations for shape (Ye, 1998) and directivity (Stanton, 1988). Generally, our resonance model formulation followed that of the prolate spheroid model described by Scoulding *et al.* (2015), apart from the calculation of the resonant frequency (5) which was taken directly from Love (1978). Resonant scattering is dependent on wavelength of incident frequency, depth range, viscosity of tissue, and size of the gas bladder (Love, 1978; Davison *et al.*, 2015; Kloser *et al.*, 2016). The backscattering cross-section is given by

$$\sigma_{bs} = \frac{a_{esr}^2 (\rho_w/\rho_f)^2}{(\omega_0^2/\omega^2 - 1)^2 + \delta^2(\omega, a, b, \xi; \Omega)} D(k, a, \theta, \sigma), \qquad (4)$$

where ω_0 is the angular resonant frequency found by solving

$$(\omega_0 a_{esr})^2 = C_e^2(a, b)\frac{3\gamma_a P_z}{\rho_f} + \frac{2s}{\rho_f a_{esr}(3\gamma_a - 1)}, \qquad (5)$$

a_{esr} is the equivalent spherical radius given by

$$a_{esr} = \left(ab^2\right)^{1/3}, \qquad (6)$$

where *a* and *b* are the semi-major and semi-minor axes of the prolate spheroid, respectively, and are related by the b-scaling parameter, β, given by

$$a = \frac{b}{\beta}, \qquad (7)$$

ω is the angular incident frequency, δ is a damping factor, ρ_f is flesh density, ρ_w is water density, *s* is the surface tension, *D* is the

Table 1. Resonance model parameter values for gas-filled swimbladders and pneumatophores (gas bladders).

Symbol	Description	Unit	Value	
ω	Incident frequency	Hz	38000	
	Damping constants (Ω)			
ρ_a	Density of air	kg m^{-3}	1.3 (Love, 1978)	
γ_a	Ratio of specific heat for air	–	1.4 (Love, 1978)	
c_{pa}	Specific heat at constant pressure for air	cal kg^{-1}°C^{-1}	240 (Love, 1978)	
κ_a	Thermal conductivity of air	cal m^{-1} s^{-1}°C^{-1}	5.5×10^{-3} (Love, 1978)	
c_w	Sound speed in sea water	m s^{-1}	1500	
ρ_w	Density of sea water	kg m^{-3}	1027	
	Gas bladder parameters		Swimbladder	Pneumatophore
θ	Mean orientation angle	degrees	0[a]	0[a]
σ	Standard deviation of orientation angle	degrees	30[a]	30[a]
z	Depth	m	Variable	525 (Proud *et al.*, 2017)
ρ_f	Tissue density	kg m^{-3}	1050 (Love, 1978)	1030 (Lavery *et al.*, 2007)
ξ	Dynamic viscosity	kg m^{-1} s^{-1}	Variable	4/3[b] (Scoulding *et al.*, 2015)
β	b-scaling parameter	–	0.64 (Yasuma *et al.*, 2010)	0.36 (Barham, 1963)
s	Surface tension at gas cavity-tissue interface	N m^{-1}	32 (Love, 1978)	0.074[c] (Love, 1978)

Comments are referred to using letters.
[a]At 38 kHz, orientation does not significantly affect backscatter of small targets (Scoulding *et al.*, 2015).
[b]In the absence of any measurements, we used the mean value from Scoulding *et al.* (2015).
[c]Surface tension of a gas bubble.

directivity function (Stanton, 1988) averaged over a normal distribution of orientation angles, $N(\theta, \sigma)$, k is the wave number, C_e is a spheroidal elongation factor (Strasberg, 1953; Weston, 1967), γ_a is the specific heat ratio for gas, P_z is pressure at depth ($P_z = z/10 + 1$, where z is depth in meters), ξ is the dynamic viscosity and Ω is a set of damping constants (Table 1). All constants used in this study are given in Table 1.

Using the constants in Table 1, σ_{bs} for a gas-bladdered fish or siphonophore, can be predicted when a_{esr} and z of the gas bladder are known. Swimbladder volume of a fish, V_{swb}, is related to a_{esr} by

$$a_{esr} = \left(\frac{3V_{swb}}{4\pi}\right)^{1/3}. \qquad (8)$$

The proportion of fish body volume, p_{swb}, can be used to calculate

$$V_{swb} = p_{swb}V_f, \qquad (9)$$

where V_f is the volume of the fish, given by

$$V_f = \frac{\frac{4\pi l_f}{2}\left(\frac{l_f}{2\alpha}\right)^2}{3}. \qquad (10)$$

Here α is the fish aspect ratio

$$\alpha = \frac{l_f}{w_f}, \qquad (11)$$

where fish shape has been approximated by a prolate spheroid and l_f (mm) and w_f (mm) are the length and width of the fish, respectively. Therefore, for a given l_f, α and p_{swb} value, a_{esr} can be estimated using (8–10), converted to a and b values, using (6 and 7), for a given b-scaling factor (β, Table 1), and used to predict

$$\sigma_{bs}(a, b, z, \xi) \cong \sigma_{bs}(l_f, p_{swb}, \alpha, z, \xi), \qquad (12)$$

from (4). Note that in (12), the constants defined in Table 1 have been omitted for clarity.

Fish weight (W_f, kg) can then be calculated by multiplying fish volume by density and is given by

$$W_f = V_f\rho_f, \qquad (13)$$

and is therefore a function of length and aspect ratio.

Mesopelagic echoes

The gas bladders of fish and siphonophores produce backscatter that contributes to 95% or more of the organisms' target strength [$TS = 10\log_{10}(\sigma_{bs})$, dB re 1 m^2, Maclennan *et al.*, 2002] when insonified at 38 kHz, the frequency used in this study. This proportion may be substantially >95% at certain specific depth-size combinations when resonant backscattering is provoked (Davison *et al.*, 2015) increasing the organisms' *TS* by a factor of 10 or more (Figure 3, see also Kloser *et al.*, 2016).

Other large mesopelagic organisms such as squid, which are likely to have similar global abundances to fish (Clarke, 1996), and medusae, have similar, low *TSs* as the bodies (flesh/bone) of fish (Figure 3) and, as with the bodies of fish, are likely to produce a relatively small proportion of total s_a (fish bodies might contribute just 5% or less: Foote, 1980; Forland *et al.*, 2014).

Smaller organisms such as copepods, although much more numerically abundant than fish, have *TS* values that are up to c. 9 orders of magnitude below that of gas-filled structures (Figure 3) so even huge densities of these organisms will not contribute significantly to the total backscatter. For example, even a preposterously high mean global copepod density of 1 million individuals per m^2 and a size distribution of $N(\mu = 2\,\text{mm},\ \sigma = 0.5\,\text{mm})$ would equate to a contribution of <1% of the predicted global mesopelagic s_a.
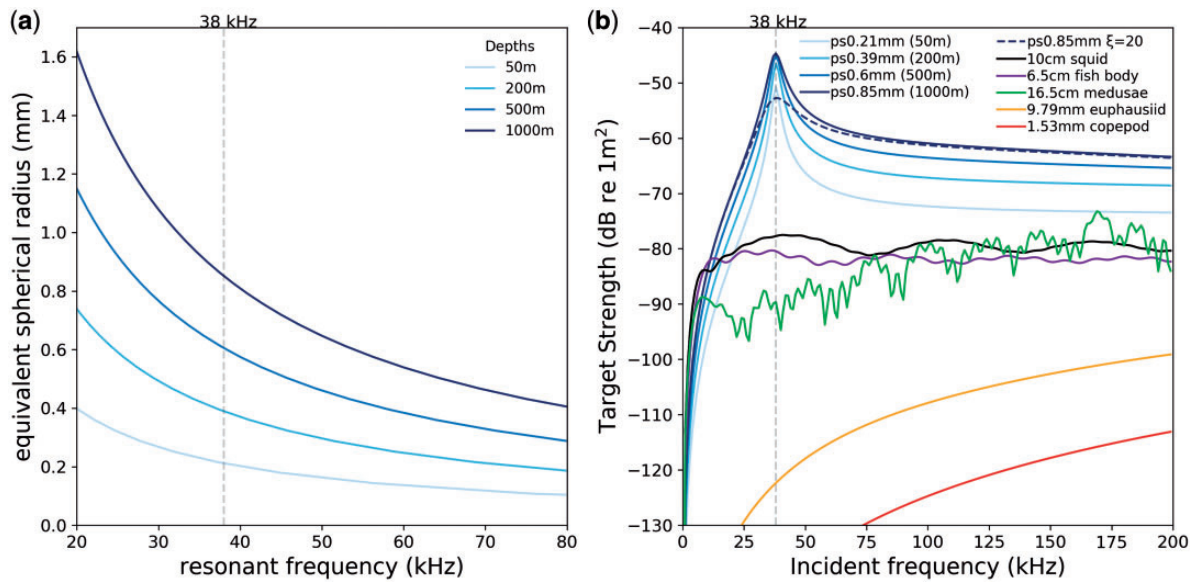
Figure 3. Dominant mesopelagic scatterers and resonance (a) A resonance model (Love, 1978) was used to predict resonant frequency of gas-filled prolate spheroids (ps—approximate shape of inflated fish swimbladders and siphonophore pneumatophores) over a range of sizes and depths; (b) TS values predicted using the resonance model for a prolate spheroid over a range of depths, where size (equivalent spherical radius) was selected to produce resonant backscattering at 38 kHz. Damping (ξ) for prolate spheroid was set to 0, except for the 0.85 mm ps at 1000 m (dashed line) where $\xi = 20$ (Love, 1978). A DWBA model (Chu *et al.*, 1993) was used to predict frequency response of a fish body (width = 1.63 cm, density contrast $g = 1.023$, sound-speed contrast $h = 1.032$), squid (width = 1.2 cm, $g = 1.043$, $h = 1.053$), medusae ($g = 1.009$, $h = 1.0004$), copepod ($g = 1.058$, $h = 1.02$) and euphausiid ($g = 1.016$, $h = 1.019$). Sizes (lengths) are given in the plot. Sound-speed and density contrast values taken from Lavery *et al.* (2007).

In summary, we assume that backscatter from gas bladders of fish and siphonophores (gas-bearing organisms) produces close to 100% of mesopelagic s_a (Lavery *et al.*, 2010; Irigoien *et al.*, 2014; Davison *et al.*, 2015). This agrees with measurements from a lowered probe that attribute 95% of the scattering at 38 kHz to gas bladders, many in resonance (Kloser *et al.*, 2016).

From individuals to populations

The previously defined equations for σ_{bs} are applicable only to individuals. To estimate global mesopelagic fish biomass, mean fish population σ_{bs} values are needed, which require fish-length distributions. We determined these as follows. We first defined a log-normal distribution:

$$X \sim \ln\mathcal{N}\left(\mu = 0, \sigma_X^2\right), \qquad (14)$$

where X is a random variable for which the mean $\mu = 0$ and the variance $\sigma^2 = \sigma_X^2$. This distribution describes the shape of the fish-length distribution and can be varied by changing a single parameter, σ_X^2.

A number sequence was used to define N equal-width fish length–frequency-distribution classes spanning the minimum and maximum fish-length values L_{min} and L_{max}:

$$L = \text{range}(a = L_{min}, b = L_{max}, c = N), \qquad (15)$$

where range(a, b, c) is a function, producing a sequence of numbers starting from a and ending with b, with total length c. Similarly, for a given σ_X^2, the log-normal distribution range was defined:

$$L_d = \text{range}(ppf_X(0.001), ppf_X(0.999), N), \qquad (16)$$

where ppf_X is the percent point function of X, and L_d and L are equal in length.

Backscattering cross-section, σ_{bs}, values were calculated for each length class and by integrating over the probability density function (pdf) of distribution X, using the trapezium rule, the population mean σ_{bs} was estimated

$$\overline{\sigma_{bs_f}} = \sum_{i=1}^{N-1} \frac{\left(\sigma_{bs_i} + \sigma_{bs_{i+1}}\right)}{2} \frac{\left(p_X(X_i) + p_X(X_{i+1})\right)}{2} (X_{i+1} - X_i)\phi_i, \qquad (17)$$

where p_X is the pdf of X and σ_{bs_i}, and ϕ_i are the σ_{bs} value and statistical weight of the ith length class, respectively. The length class weight, ϕ_i, is included to enable the relative contribution of each length class (i.e. proportion of class with gas bladders) to $\overline{\sigma_{bs_f}}$ to be varied. Similarly, mean population weight is given by

$$\overline{W_f} = \sum_{i=1}^{N-1} \frac{\left(W_{f_i} + W_{f_{i+1}}\right)}{2} \frac{\left(p_X(X_i) + p_X(X_{i+1})\right)}{2} (X_{i+1} - X_i). \quad (18)$$

Here, the statistical weighting is absent because all fish will contribute to the mean population weight, regardless of whether they possess a gas bladder or not.

Mesopelagic fish biomass model

The backscatter from fish and siphonophores was assumed to produce the majority of mesopelagic s_a—a reasonable assumption given Figure 3. Therefore, simplified total area-backscattering

coefficient $s_a{}^*$ is the sum of the contributions of backscattering from siphonophores and fish:

$$s_a{}^* = (p_f + p_{siph})s_a, \qquad (19)$$

where p_f and p_{siph} are the proportion of s_a produced by fish and siphonophores, respectively.

Substituting (17 and 18) into (2), mesopelagic fish biomass, for a global population, is estimated using

$$B_f = A \frac{s_a^f}{\overline{\sigma_{bs_f}}(\sigma_X^2, \alpha, p_{swb}, z, \xi)} \overline{W_f}(\sigma_X^2, \alpha), \qquad (20)$$

where s_a^f is the amount of s_a produced by fish ($p_f s_a$).

Model scenarios

All myctophids (a very common and abundant mesopelagic fish) are thought to develop swimbladders during development (Bone *et al.*, 1995; Moser, 1996) and some species of mesopelagic fish are known to keep their swimbladders throughout their lifecycles (e.g. marine hatchetfish). Myctophids caught in the Tasman sea region were found mostly to have gas bladders (Flynn and Pogonoski, 2012) but mesopelagic fish in general have often been reported to have varied swimbladder states, including absent, uninflated, and inflated (Butler and Pearcy, 1972; Neighbors and Nafpaktitis, 1982; Bardarson, 2013), often reported to be linked to ontogeny, where juveniles or young adults possess uninflated or absent swimbladders (Yasuma *et al.*, 2010) and late-stage adults have reduced (fat invested) swimbladders (Butler and Pearcy, 1972; Neighbors and Nafpaktitis, 1982).

To examine the impact of the observed variability in swimbladder state on acoustically inferred biomass of a global mesopelagic fish population, three scenarios were investigated. Scenario 1 (S1), had equally weighted length classes ($\phi = 1$, see Equation 17), i.e. all fish had gas bladders. In scenario 2 (S2), ϕ followed a cosine function (i.e. the smallest length classes always had gas bladders), given by

$$\phi_i = \begin{cases} \phi_{min} + \cos\left(L_i - L_{min}(90/(L_{97.5} - L_{min}))\right)(1 - \phi_{min}), \\ \qquad\qquad\qquad\qquad\qquad\qquad\qquad L_i < L_{97.5} \\ \phi_{min}, \qquad\qquad\qquad\qquad\qquad\qquad L_i \geq L_{97.5}, \end{cases} \qquad (21)$$

where i is the length class index, ϕ_{min} is a constant ranging between 0 and 1 and denotes the minimum proportion of fish per length class with gas bladders (i.e. the proportion of fish that do not lose their gas bladders with age) and $L_{97.5}$ is the length at the 97.5th percentile of the cumulative distribution function (Figure 4a); the 97.5th percentile was chosen to avoid fitting the cosine curve to extensive tails in the log-normal distributions. In effect, the rate of decay of the curve was controlled by the value of ϕ_{min}. For scenario 3 (S3), ϕ was scaled to a sine curve, similar to the shape observed by Yasuma *et al.* (2010) for *Myctophum asperum*, over the population length range:

$$\phi_i = \sin(L_i - L_{min}(90/(L_{cent} - L_{min}))), \qquad (22)$$

where the maximum value of the sine function angle was set to 180 degrees and L_{cent} is the length at the centre of the pdf where
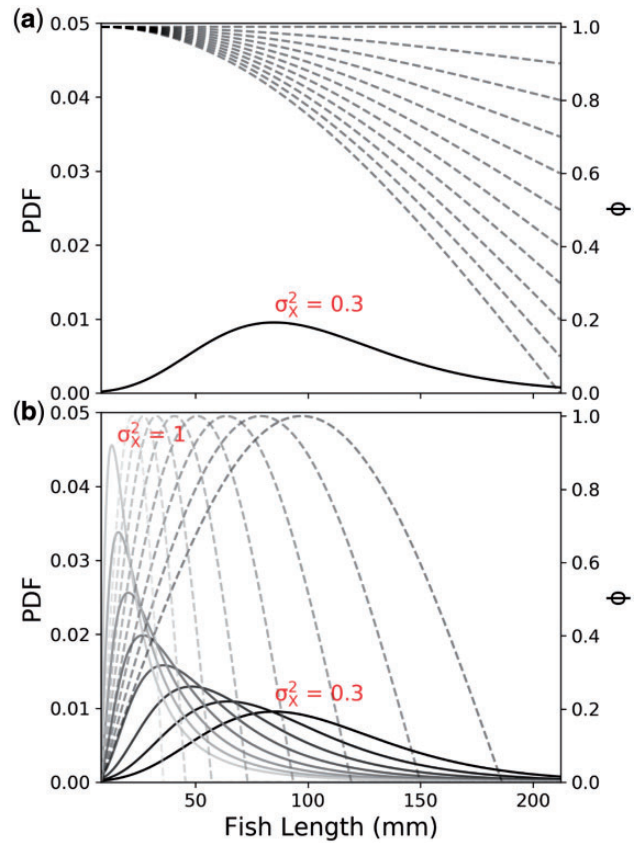
Figure 4. Length class weighting (ϕ; proportion of gas-bladdered fish by length class, shown by dashed line) for scenarios 2 (a) and 3 (b). (a) Single log-normal distribution plotted ($\mu = 0$, $\sigma_X^2 = 0.3$), ϕ is plotted over a range of ϕ_{min} values between 0 and 1. (b) Log-normal distributions scaled to fish length class, where the mean was set to 0 and the variance (σ_X^2) ranged from 0.3 to 1. ϕ plotted for each distribution. Maximum value of x-axis set to $L = 212$ mm, which is the length class at the 97.5th percentile of the broadest log-normal distribution ($\mu = 0$, $\sigma_X^2 = 0.3$).

the cumulative distribution function equalled 0.5 (Figure 4b). This ensured that a large proportion of small (young) and large (old) fish were without gas bladders and that the proportion with gas bladders increased towards the centre of the distribution.

Model input parameters

To predict mesopelagic fish biomass (B_f, 20) for scenarios 1–3, uniform distributions were assumed for each model variable (s_a^f, σ_X^2, α, p_{swb}, z, ξ, Table 2). Scenario 2 also included ϕ_{min}, the minimum proportion of gas-bladdered fish per length class, which was also assumed to have a uniform distribution, with minimum and maximum values of 0 and 1, respectively (Figure 4a). The parameter values have the potential to be widely variable but at present we do not have enough knowledge to predict accurately their global distributions. Here, we use uniform distributions to ensure that we capture the full range of variability that they could potentially contribute to global mesopelagic fish biomass. These parameters and their corresponding distribution ranges were chosen based on the following reasoning.

Table 2. Assumed fish population input parameter statistical distributions.

Symbol	Description	Unit	Distribution
s_a^f	Mesopelagic fish area-backscattering coefficient	$m^2\,m^{-2}$	U(0, 2.38 × 10^{-5}) (Proud et al., 2017)
σ_X^2	Variance of length distribution	–	U(0.3, 1)
α	Aspect ratio of fish body	–	U(4, 12)
p_{swb}	Swimbladder volume as a proportion of fish volume	–	U(0.0001, 0.0263) (Yasuma et al., 2010)
z	Depth, z	m	U(200, 1000)
ξ	Dynamic viscosity	$kg\,m^{-1}\,s^{-1}$	U(0, 20) (Love, 1978)
ϕ_{min}	Minimum proportion of gas-bladdered fish per length class used in scenario 2	–	U(0, 1)

Distribution of each parameter is given (U, uniform distribution).

There are few reported open-ocean observations of siphonophore density or pneumatophore size distributions. Pneumatophores have been reported to have mean lengths ranging between 0.15 mm (Lavery et al., 2007) and 3.27 mm (Barham, 1963), and densities from <1 to >1000 individuals m^{-2} (Mackie et al., 1988). Considering the lack of information, p_{siph} might reasonably be considered to vary from place to place anywhere between 0 and 1, i.e. siphonophores potentially could produce almost all or none of the total mesopelagic s_a. Mesopelagic fish s_a, s_a^f, was drawn from a uniform distribution, where the minimum value was set to 0 (for the case where $p_{siph} = 1$, Equation 19) and maximum value of 2.38 × 10^{-5} m^2 m^{-2}, the upper bound (mean plus RMSE) taken from Proud et al. (2017).

The variance of the log-normal distributions, σ_X^2, was varied uniformly between 0.3 and 1. The distribution ranges were then matched with the fish population length range (15), where L_{min} and L_{max} were set to 8 mm (approximately the size of a newly developed juvenile myctophid; Moser, 1996) and 315 mm (maximum reported length of any species in the family Myctophidae, www.fishbase.org), respectively, to yield length distributions (Figure 4). As σ_X^2 was increased from 0.3 to 1, the length distribution shifts from a gaussian-like distribution ($\mu = c$. 88 mm, equal to the median asymptotic length of 219 species of myctophid from www.fishbase.org) to a population dominated by smaller (more likely to produce resonant backscatter) fish, as commonly observed (e.g. Davison et al., 2015). Although L_{max} was set to 315 mm, the effective maximum length of the fish population was closer to 212 mm (97.5th percentile of broadest log-normal distribution, see Figure 4), which is similar to the 97.5 percentile of the asymptotic lengths of all documented myctophid species (c. 211 mm, www.fishbase.org). For the length distributions used in this study (Figure 4), the majority of fish were smaller than 88 mm, which is consistent with the sizes of common taxa of mesopelagic fish (e.g. Gonostomatidae, Sternoptychidae, Myctophidae, and Phosichthyidae) known to have gas bladders (Marshall, 1971; Bone et al., 1995; Flynn and Pogonoski, 2012).

The aspect ratio, α, a representation of variability in species morphology within the population, was varied uniformly between 4 and 12 (Flynn and Pogonoski,, 2012). Changes in α impact both fish mean weight and swimbladder volume (9–13).

During diel vertical migration (DVM), the gas bladders of fish and siphonophores undergo compression on descent and expansion on ascent, following Boyle's Law. Some species inflate their gas bladders and follow a "constant buoyancy strategy," whilst others do not, and swim to maintain depth (Denton, 1961; Hersey et al., 1962; Kalish et al., 1986; Thompson and Love, 1996; Love et al., 2003, 2004; Scoulding et al., 2015); this behaviour is likely to vary between and within species, and ontogenetically. Our uncertainty around gas bladder function during and between bouts of DVM stems from the difficulty in making measurements of gas bladder volume at the surface. Bladders of fish brought to the surface from depth may be excessively distended or ruptured following rapid decompression and the measured volumes may not be good indicators of actual volumes in situ at depth. Because of this uncertainty, gas bladder volume as a proportion of body size, p_{swb}, was varied between 0.0001 and 0.0263, equivalent to 0.01 and 2.63% of body volume (Yasuma et al., 2010). The maximum value of p_{swb} is likely to be limited by neutral buoyancy (body density), which does vary with length for many species (Butler and Pearcy, 1972; Neighbors and Nafpaktitis, 1982; Davison, 2011b). The range of values chosen, result in a broad range of V_{swb} values (9), which include proportions, both small, representative of gas bladders that do not re-inflate when compressed at depth, and larger proportions, which are consistent with gas bladder sizes required to maintain neutral buoyancy.

Fish (or DSL) depth, z, was varied uniformly in the model between 200 and 1000 m. This parameter affects the resonant frequency (5). For a given gas bladder size, the resonant frequency increases with depth; during DVM, a change in depth will cause a change in gas bladder volume, and this variability is captured by other model parameters (primarily by p_{swb}) not by depth.

Dynamic viscosity, ξ, (i.e. the viscosity of the gas bladder wall) was set to vary uniformly between 0 kg m^{-1}s^{-1}, i.e. no damping, resulting in a sharp resonance peak (as might be expected from a gas bubble) up to a value of 20 kg m^{-1}s^{-1}, which completely dampens the resonance peak (Figure 3). The latter value is as suggested by Love (1978) for midwater fish. There is some contention around this parameter and its validity in modelling the TS of resonant gas bladders (Baik, 2013). Here, we included a broad range of ξ values to ensure that we captured both undamped and damped resonant behaviour in our estimates of global mesopelagic fish biomass.

Estimates of global mesopelagic fish biomass

A joint probability distribution (J) was defined from the six (seven in the case of scenario 2) uniform distributions of the input parameters defined in Table 2. For a single model run, 5000 samples were generated from J using the quasi-random Sobol sequence (Sobol, 1967): this provides a more evenly distributed sample set in parameter space than a purely random sample. Sample estimates of mean fish population σ_{bs}, mean fish W, and global mesopelagic fish biomass were generated using (17, 18, and 20), respectively, for all three scenarios. Uncertainty in biomass estimates was quantified using summary statistics, and is presented by box plots in Figure 5.
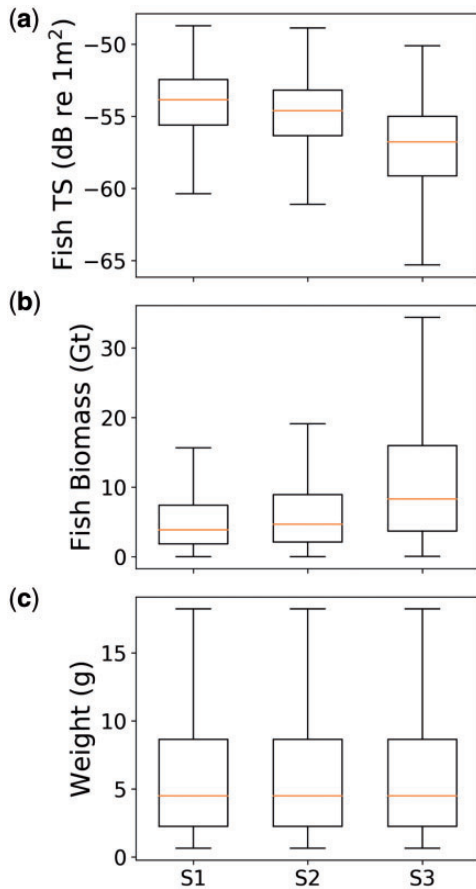
Figure 5. Summarized mesopelagic fish biomass model results for each scenario. (a) Mean fish $TS = 10\log_{10}(\overline{\sigma_{bs_f}})$, (b) global fish biomass, and (c) mean individual fish weight. Scenario 1 (S1) all fish have gas bladders, whereas in scenarios 2 (S2) and 3 (S3), a proportion of fish are without gas bladders. Horizontal line within each box is the median value, box limits are the inter-quartile range, i.e. 25 and 75% quantiles. The whiskers (vertical lines) are 1.5 times the inter-quartile range. Outliers not plotted.

Three additional model runs were performed in which s_a^f was set to the upper (2.38×10^{-5} m² m⁻²), lower (1.5×10^{-5} m² m⁻²) and mean (1.94×10^{-5} m² m⁻²) values of global mesopelagic s_a from Proud *et al.* (2017), to determine a range of maximum mesopelagic fish biomass estimates, i.e. the contribution of siphonophores to global mesopelagic s_a was assumed to be zero. The maximum values of B_f were scaled between 0 and 100% and compared with potential contribution of siphonophores to mesopelagic s_a (p_{siph}, 19), predicted over a range of siphonophore mean global densities (ρ_{siph}, 0.1–1000 inds m⁻², uniform) and gas bladder size distributions $\{a_{siph}$ (mm) $\sim N[\mu = U(0.3, 5), \sigma = \mu/3.5]\}$, where p_{siph} is given by

$$p_{siph} = \frac{\rho_{siph}\overline{\sigma_{bs}(a_{siph}, b, z, \xi)}}{s_a^f}, \qquad (23)$$

where $z = 525$ m the global mean DSL value (Proud *et al.*, 2017), $\xi = 4/3$ (mean from Scoulding *et al.*, 2015) and b was calculated using βa_{siph} (7), using a β value of 0.36 (Barham, 1963).

Sensitivity of input parameters

A global sensitivity analysis was conducted using a variance based sensitivity metric (Saltelli *et al.*, 2010) to investigate how the different input parameters of the biomass model affected the total biomass. The total effect index is a sensitivity metric that captures both the first order effect as well as higher order effects (interactions). The total effect index for parameter X_i is given as

$$S_{Ti} = \frac{E_{X_{\sim i}}(V_{X_i}(B_f|X_{\sim i}))}{V(B_f)}, \qquad (24)$$

where $V_{X_i}(B_f|X_{\sim i})$ is the variance of the biomass estimate when changing the input parameter, X_i, $E_{X_{\sim i}}$ is the mean of $V_{X_i}(B_f|X_{\sim i})$ and $V(B_f)$ is the total variance of the model. The inner variance estimator captures the variance in the biomass while varying X_i and the outer mean operator takes the mean of these variances.

We used simulations to estimate the sensitivity indices. The total effect index

$$S_{Ti} = \frac{\frac{1}{2N}\Sigma_{j=1}^{N}\left(B_f(\boldsymbol{C})_j - B_f(\boldsymbol{C_D^i})_j\right)^2}{V(B_f)} \qquad (25)$$

is estimated using the Jansen (1999) estimator (Saltelli *et al.*, 2010, Table 2). Here, N is the number of simulations, $\boldsymbol{C}$ is a set of N sets of parameters drawn from a Sobol sequence (rows are realizations j and columns are the parameter i), $\boldsymbol{C_D^i}$ is identical to $\boldsymbol{C}$ except that parameter i is replaced from a similar but independent resampling set $\boldsymbol{D}$. S_{Ti} was calculated for 100 model runs, where for each run, N was set to 5000.

Results

A fish biomass model was constructed and parametrized by seven input factors (s_a^f, σ_X^2, α, p_{swb}, z, ξ, ϕ_{min}, the latter of which was used only in scenario 2, see Table 2 for definitions) and run for three different scenarios: S1, which assumed the fish population was comprised solely of fish with gas bladders; S2 where all fish had gas bladders as juveniles, and a minimum proportion of fish kept their gas bladders throughout their life, whilst a growing proportion (following a cosine curve) lost their gas bladder with increasing length, and S3, a population with a large proportion of small and large fish without gas bladders. Five thousand biomass estimates were generated for each model run to capture the range of possible variability and so illustrate uncertainty (Figure 5).

Fish biomass uncertainty

Model results for S1–S3 were summarized using box plots (Figure 5). Median values of TS decreased from -53.8 dB re 1 m² (lower quartile, Q1 $= -55.6$; upper quartile, Q3 $= -52.4$) to -56.8 dB re 1 m² (Q1 $= -59.1$; Q3 $= -55$) and median biomass increased from 3.833 Gt (Q1 $= 1.812$; Q3 $= 7.374$) to 8.292 Gt (Q1 $= 3.670$; Q3 $= 15.962$) from S1 to S3. Since the proportion of gas-bladdered fish per length class has no impact on fish weight, it was constant for all three scenarios and had a median value of 4.51 grams (Q1 $= 2.25$; Q3 $= 8.64$).

Maximum fish biomass and contributions of fish and siphonophores to global mesopelagic backscatter

Maximum mesopelagic fish biomass was estimated for each scenario. The minimum lower (25%) and maximum upper (75%)

Table 3. Median mesopelagic fish biomass predictions (Gt) by siphonophore contribution for each scenario.

Scenario	Siphonophore contribution (%)										
	0	10	20	30	40	50	60	70	80	90	99
1	7.082	6.373	5.665	4.957	4.249	3.541[a]	2.832[a]	2.124[b]	1.416[c]	0.708[c]	0.071
2	8.588	7.729	6.870	6.012	5.153	4.294	3.435[a]	2.576[a,b]	1.718[c]	0.859[c]	0.086
3	15.255	13.729	12.204	10.678	9.153	7.627	6.102	4.576[a]	3.051[a,b]	1.525[c]	0.153[c]

[a]Value range that includes mesopelagic fish biomass calculated for a trophic efficiency of 10% per trophic level (3.363 Gt, see Figure 6).
[b]Value closest to a food-web model estimate of mesopelagic fish biomass (2.4 Gt, Anderson et al., 2018).
[c]Value range that includes mesopelagic fish biomass predicted by ocean trawls (1 Gt, Gjøsaeter and Kawaguchi, 1980) and total consumer biomass by a macro-ecological model (1.4 Gt, Jennings and Collingridge, 2015).

quartiles from the maximum fish biomass estimates for all three scenarios were used to represent the range of maximum mesopelagic fish biomass assuming that siphonophores made no contribution towards global daytime mesopelagic DSL backscatter. The maximum values were then scaled between 0 and 100% to yield fish biomass estimates for different global mean densities and gas bladder size distributions of siphonophores (Figure 6 and Table 3). Fish biomass values were calculated for TE values of 5, 10, and 20% per trophic level to be 0.732, 3.363, and 15.453 Gt, respectively, and were plotted in Figure 6.

For any given siphonophore density and gas bladder size distribution, global fish biomass values can be predicted for each gas bladder scenario using Figure 6, e.g. for a global population of siphonophores with normally distributed gas bladder lengths with a mean < 0.6 mm (e.g. as in Lavery et al., 2007), equivalent to a a_{esr} of c. 0.15 mm (6 and 8), fish biomass would make up close to 100% of mesopelagic s_a for any given mean global density of siphonophores (<1000 individuals m^{-2}). Conversely, for a mean gas bladder a_{esr} larger than 1 mm (e.g. Barham, 1963; Pickwell, 1966), siphonophores are dominant, contributing almost 100% of mesopelagic s_a for a given mean open-ocean siphonophore density, larger than c. 6.5 individuals per m^2 (e.g. Robison et al., 1998).

At 10% TE per trophic level, mesopelagic fish biomass is c. 3.363 Gt (Figure 6)—a value which falls between a fish contribution of 40 and 50% under S1, between 30 and 40% for S2 and between 20 and 30% for S3 calculated from model median fish biomass values (Table 3). Non-acoustic estimates of global mesopelagic fish biomass (Gjøsaeter and Kawaguchi, 1980; Jennings and Collingridge, 2015; Anderson et al., 2018) suggest that the contribution of siphonophores to total mesopelagic backscatter may be 50% or more (Table 3).

Sensitivity analysis

The total effect index S_{Ti} was calculated for input parameters used in the maximum fish biomass model run for each scenario (Figure 7). The area-backscattering coefficient for mesopelagic fish, s_a^f was set to the global mean value, 1.94×10^{-5} m^2 m^{-2} (Proud et al., 2017). This constraint was applied because the model would be very sensitive to a distribution that varies the total s_a^f value between 0 and the maximum value, 2.38×10^{-5} m^2 m^{-2}; including s_a^f as a distribution rather than a constant in the sensitivity analysis leads to unclear results, as S_{Ti} for s_a^f tends to 1 and the values for the other parameters are very small. For scenarios S1 and S2, the results show that swimbladder volume (as a proportion of body size), p_{swb}, is the most important parameter, followed by the aspect ratio, α, and length distribution parameter, σ_X^2. Fish depth (z) and viscosity (ξ),

affecting the resonant frequency (5) and damping of the resonant peak (Equation 4 and Figure 3), respectively, contribute relatively little to the overall model uncertainty. At an individual level, these parameters are very important (Scoulding et al., 2015) but this importance reduces substantially when considering the full range of the parameter space, which includes, for example, variability in population structure (e.g. shape of length-frequency distribution). For S3, p_{swb}, and σ_X^2 are the most important parameters, i.e. α has a reduced impact on model uncertainty.

Discussion

By exploration of likely echo energy levels arising from mesopelagic organisms, characterized using acoustic scattering models, it became apparent that siphonophores and fish were likely to be the dominant scatterers in the mesopelagic zone during the daytime (Figure 3). Our model results predict a range of global mesopelagic fish biomass values between 1.812 (lower quartile of S1) and 15.962 Gt (upper quartile of S3). The median biomass value of S1, 3.833 Gt, is our equivalent of a previous median acoustic biomass estimate of between 14.3 and 19.5 Gt (Irigoien et al., 2014, extrapolated from those authors' 40° S to 40° N geographical range, to "our" 70° S to 70° N range). Our lower values are a consequence of acknowledging that a proportion of the total acoustic backscatter is resonant (high intensity echoes from low biomass targets), that siphonophores contribute to the total backscatter, and the uncertainty in population characteristics (i.e. species' morphology and length distribution). For S3, where the proportion of gas-bladdered fish is reduced for small and larger fish, our prediction of median biomass of 8.292 Gt differs from Irigoien et al. (2014) by only a factor of two. Due to escapement and avoidance, the global biomass estimate by trawling of 1 Gt (Gjøsaeter and Kawaguchi, 1980) could be out by factor of seven or more (Koslow et al., 1997; Kloser et al., 2009; Yasuma and Yamamura, 2010; Davison, 2011a), which allows a prediction of c. 7 Gt or more: that is very close to the median value of S3. Conversely, a recent simple food-web model predicted mesopelagic fish biomass to be just 2.4 Gt (Anderson et al., 2018), which is within the biomass ranges of S1 and S2. Considering that S2 is probably the more likely of our scenarios (Butler and Pearcy, 1972; Neighbors and Nafpaktitis, 1982; Davison et al., 2015), the uncertainty in our acoustic derived estimate could be reduced to between 2.091 and 8.903 Gt (lower quartile to upper quartile). This range also overlaps with the range derived using a macroecological model, i.e. a median biomass of 1.4 Gt for all consumers, with 95th percentile of 8.1 Gt (Jennings and Collingridge, 2015).
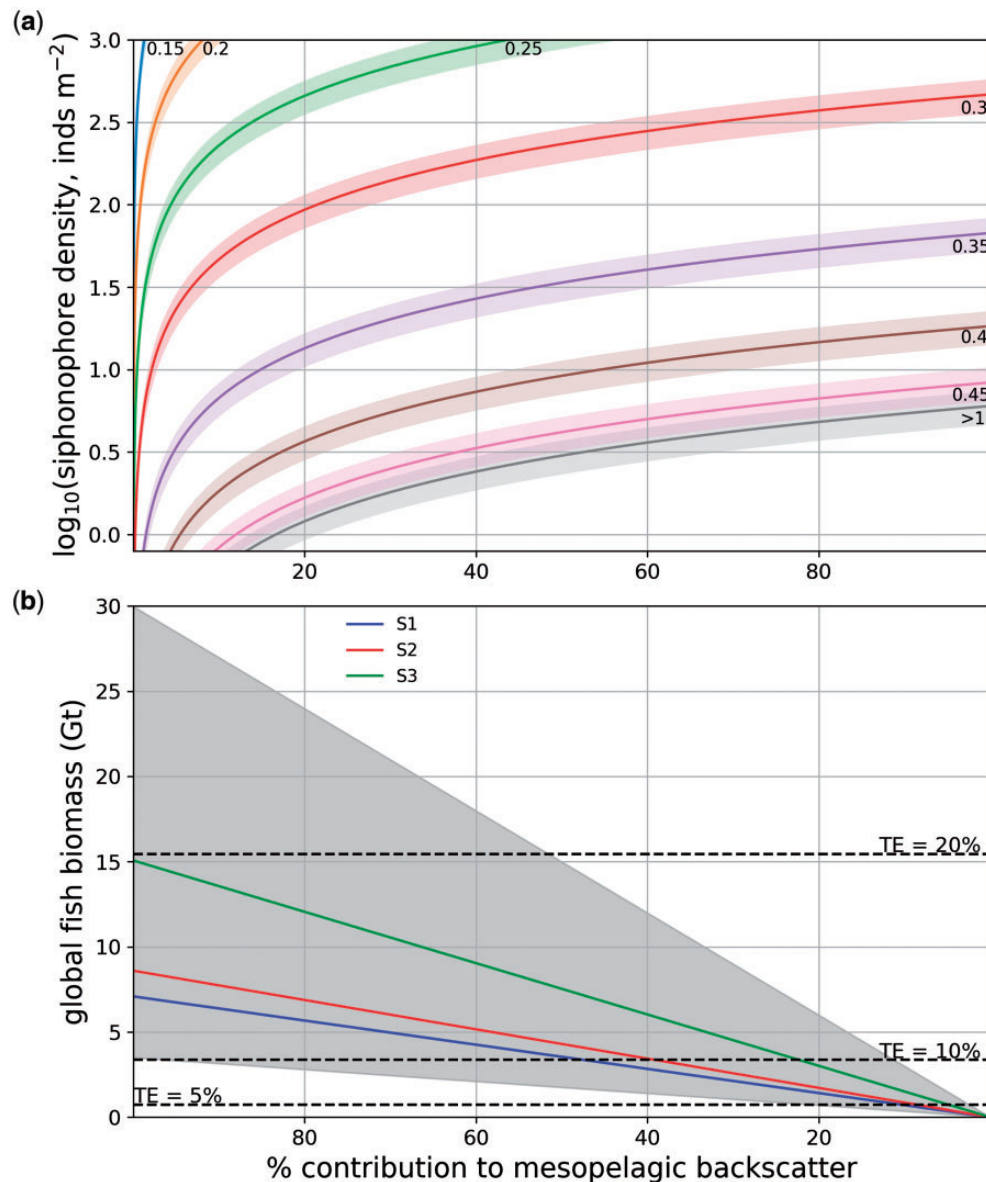
Figure 6. Relative contributions of fish and siphonophores to global mesopelagic area-backscattering coefficient, over a range of siphonophore mean global densities and gas bladder size distributions. (a) Each line represents a separate mean gas bladder equivalent spherical radius (a_{esr}, labelled in mm). Shaded region calculated from global mesopelagic area-backscattering coefficient RMSE from Proud *et al.* (2017). Mean a_{esr} values larger than 1 mm can be approximated by the line labelled ">1." (b) Shaded region spans the upper (75%) quartile of S3 and the lower (25%) quartile of S1 (3.495–29.975 Gt), calculated using results of the maximum fish biomass model run. Coloured lines are median values for each scenario. TE (per trophic level) between phytoplankton and mesopelagic fish estimated from Gascuel *et al.* (2008) using a mean water temperature of 7.2°C and PP value of 0.312 g C d^{-1} (Proud *et al.*, 2017) are indicated by dashed lines.

Model sensitivity

Given that the relative proportions of fish and siphonophore backscatter are known, swimbladder volume (as a proportion of body size), p_{swb}, was the most sensitive parameter in the mesopelagic fish biomass model for all three scenarios (Figure 7). This is not surprising, since the gas bladders of mesopelagic fish are predominantly smaller than the wavelength of sound at 38 kHz (c. 4 cm) and therefore volume, not shape or orientation, drives *TS* (i.e. Rayleigh scattering, see Figure 1). Other parameters in the model, such as the aspect ratio (α) and distribution variance (σ_X^2) were also important (Figure 7). To reduce the uncertainty caused

by p_{swb} in the model, we must first resolve the issue of compression during DVM, i.e. do fish inflate their bladders at depth (constant buoyancy strategy), to remain neutrally buoyant, or not? Evidence in the literature is mixed (Denton, 1961; Hersey *et al.*, 1962; Kalish *et al.*, 1986; Thompson and Love, 1996; Love *et al.*, 2003, 2004; Scoulding *et al.*, 2015). The problem can only be solved by making more observations of the mesopelagic community at depth, using for example, paired optical/acoustic systems (e.g. Marouchos *et al.*, 2016), which will improve our knowledge and help narrow the distributions of the other model parameters.
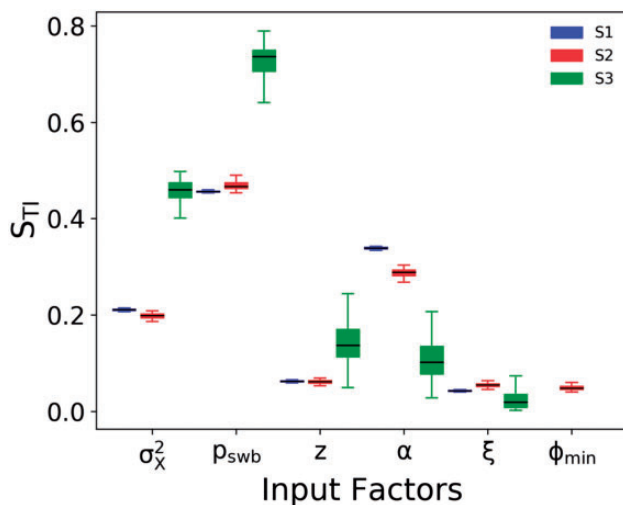
Figure 7. The total effect index S_{Ti} of the mesopelagic fish biomass model input parameters for scenarios S1–S3: distribution variance (σ_X^2), swimbladder volume as a proportion of body volume (p_{swb}), depth (z), aspect ratio (α), dynamic viscosity of gas bladder wall (ξ), and minimum proportion of gas-bladdered fish (ϕ_{min}). In this model run, mesopelagic fish s_a, s_a^f, is constant, set to the global mean value of 1.94×10^{-5} m^2 m^{-2}.

Model caveats

The mesopelagic fish biomass model (20) derived here assumes that siphonophores are the only other significant contributor to mesopelagic s_a. In most cases, this is probably a valid assumption (Barham, 1963; Lavery et al., 2007; Kloser et al., 2016) but, where fish densities are low, other scatterers such as squid and jellyfish will become more prominent (Clarke, 1996; Pauly et al., 2009; Haraldsson et al., 2012). In some instances, e.g. the polar regions, zooplankton populations may dominate (Murphy et al., 2007). At a global scale, the assumption is reasonable but to follow a similar approach as made here at regional or smaller scales, the contribution of other scatterers will need to be considered. Fortunately, our approach can readily incorporate contributions from other scatterers, indeed we started with multiple scatterers (Figure 3) and eliminated groups that contributed little to total scattering. We recommend this approach is adopted at regional scales and that results arising from such analyses are not extrapolated to other regions that likely contain different mesopelagic communities.

We made a number of assumptions when selecting model parameters and distributions (Tables 1 and 2). We depended heavily on the literature which, in most cases, describes observations made only over small spatial ranges (i.e. local studies; e.g. Neighbors and Nafpaktitis, 1982; Yasuma et al., 2010). This reflects the paucity of data concerning mesopelagic fish and siphonophores, and highlights the pressing requirement for increased sampling at depth. The validity of our analysis results is also dependent upon our present level of knowledge, which is relatively poor (St John et al., 2016). For example, the density of mesopelagic fish (ρ_f) was assumed to be 1050 kgm^{-3}, a reasonable median value taken from Love (1978). The value of ρ_f for mesopelagic fish varies between 1030 and 1080 kgm^{-3} (Capen, 1967; Butler and Pearcy, 1972; Davison, 2011b; Davison et al.,

2015). Inputting this range of ρ_f values into our biomass model did not substantially change estimates of fish biomass ($\pm 2.5\%$). However, fish with higher densities are more likely to have inflated swimbladders, and that possible interaction is not considered in our analysis. As our understanding develops and we obtain more observational data, we may need to include additional parameters into our model framework.

The largest source of uncertainty in the mesopelagic fish biomass model is the unknown contribution of siphonophore to mesopelagic s_a. It is likely that fish produce most of the backscatter at 38 kHz but the proportion remains largely unknown.

Siphonophores

A range of siphonophore densities and gas bladder sizes have been observed, from very small siphonophores in the Gulf of Maine (0.15 mm mean gas bladder length, Lavery et al., 2007) and low-density populations <1 individuals m^{-2} (Mackie et al., 1988), to large *Nanomia bijuga* in the San Diego Trough (3.27 mm length, Barham, 1963) and high densities in the east Indian Ocean (>1000 individuals m^{-2}, Musayeva, 1976). Siphonophores are often less abundant in open ocean than in neritic regions, for example Kloser et al. (2016) observed, using a lowered probe, just 2.5 individuals m^{-2} in the open Southern Ocean (Kloser et al., 2016). The total size of siphonophores varies from a few cm to several m but there is presently no understanding of how this size relates to gas bladder size at depth: variability in siphonophore size by cryptic species, population genetic variation, seasonality, or ecological conditions are also unknown (C. Dunn, pers. comm.). Against this background of uncertainty, to attribute legitimately large proportions of global mesopelagic s_a to fish biomass, one of the following must be true: (i) in the open ocean, siphonophore densities are relatively low in the mesopelagic zone; (ii) after descent to depth, during DVM, a lot of gas-bearing siphonophores are not able to re-inflate their gas bladders at the now-high ambient pressure, or (iii) the majority of siphonophore gas bladders do not produce resonant backscatter at 38 kHz in the 200–1000 m depth range (e.g. 0.4 mm > a_{esr} > 1.0 mm, Kloser et al., 2016).

Presently, we are limited to small-scale visual estimates of siphonophores, from SCUBA to ROVs and submersibles (e.g. Rogers, 1978; Robison et al., 1998); the Monterey Bay Aquarium Research Institute does have an extensive database called the Video Annotation and Reference System (VARS), which contains records of siphonophores observed in ROV dives, since before 2000 (Schlining and Stout, 2006). To reduce uncertainty in estimates of fish biomass, more data on global variability in siphonophore density and size distribution are needed.

Swimbladders

The swimbladder state (present/absent/reduced/inflated) and volume (with respect to body size) of mesopelagic fish is highly variable between species (Butler and Pearcy, 1972; Neighbors and Nafpaktitis, 1982; Yasuma et al., 2010) and within species (Scoulding et al., 2015). Swimbladder function during DVM is also not well understood (Denton, 1961; Hersey et al., 1962; Kalish et al., 1986; Thompson and Love, 1996; Love et al., 2003, 2004; Scoulding et al., 2015). It is likely that some species adopt the "constant buoyancy strategy," as observed by Barham (1971) from a submersible, where fish reside in a torpid state and remain neutrally buoyant during the daytime. The alternative is the "tread-water strategy," whereby fish maintain depth by swimming

(Love *et al.*, 2004). The trade-off between the two strategies is the energetic cost of absorption and secretion of gas, which can be high (Bone *et al.*, 1995) vs. the energetic cost of swimming to maintain depth. In addition, a fish in a torpid state, vs. a fish in constant movement, may be more difficult to detect visually, and hence, at lower risk of predation from deep-diving predators (e.g. King penguins and Elephant seals). Strategy may also change during the life cycle of mesopelagic fish, since density reduces with size (via lipid investment, e.g. Gee, 1983) and therefore, older, larger fish, are more likely to opt for the constant buoyancy strategy (Butler and Pearcy, 1972; Neighbors and Nafpaktitis, 1982; Davison, 2011b). An additional complication is that "resident" DSLs have often been observed (Figure 2) presumably containing some species that do not migrate, and the proportion of species that migrate do so seasonally with different proportions and length classes (Koslow *et al.*, 1997; Flynn and Kloser, 2012).

In the absence of any known environmental drivers of swimbladder volume and state in mesopelagic fish, our method is useful because it provides a mean view of a likely very complex system. To move forward and reduce uncertainty in estimates of mesopelagic fish biomass, a better understanding of variability at the individual level is required (e.g. *TS* variation with depth). If DVM behaviour, swimbladder state, and volume can be related to the environment, we will not only make more accurate estimates of mesopelagic fish biomass but also will gain a better understanding of how community-scale properties, such as vertical depth structure, emerge from the behaviour of individuals.

Wider implications for ecosystem models

The analysis framework developed here could be used to build an acoustic observation model (Handegard *et al.*, 2013), to predict the expected acoustic "views" of simulated ecosystems, e.g. Atlantis, SEAPODYM, MIZER, and size-based ecosystem models (Lehodey *et al.*, 2008, 2014; Fulton *et al.*, 2011; Trebilco *et al.*, 2013; Scott *et al.*, 2014), and to compare those predictions with actual acoustic observations. This would serve to provide ecosystem modellers with a method to validate the mesopelagic component of their models. This is of particular importance for ecological/biogeochemical models that simulate the biological carbon pump and provide carbon fluxes for coupled climate models (Giering *et al.*, 2014).

Moving forward

The predicted global mesopelagic s_a used here was based on 38 kHz observations (Proud *et al.*, 2017). A lot of data are available at a frequency of 38 kHz, but use of single frequency data alone does not enable frequency–response analyses that can identify scattering type (e.g. Kloser *et al.*, 2002; Lavery *et al.*, 2010). Data at 18 kHz, the only other commonly used frequency that has a high enough signal-to-noise ratio to provide useful observations from the entire mesopelagic zone, are often collected alongside 38 kHz data (www.imos.org.au). Using 18 and 38 kHz together could enable resonance peaks to be identified, and the mean size of the target to be predicted. Performed at a global scale, this would at least provide some information concerning regional-scale size structure of gas-bearing organisms.

Increased *in situ* optical and acoustic sensing in the ocean will advance the understanding of the depth distribution and abundance of siphonophores. As an example, profiling probes are being proposed (Handegard *et al.*, 2010) and developed (Kloser *et al.*, 2016). The gelatinous community (including siphonophores) is woefully under sampled and the incorporation of cameras on profiling probes will greatly increase our understanding of their distribution and abundance. In the future, combining such probes with acoustic and optical sensors could be done on a global scale in an ARGO float style of approach (Handegard *et al.*, 2010).

Concluding remarks

We used predicted global 38 kHz DSL backscattering intensity (from Proud *et al.*, 2017) to estimate global mesopelagic fish biomass. Our range of possible estimates spanned 1.812–15.962 Gt (lower and upper quartile). This range of values lends credence to the idea that there may be a substantial biomass of fish in the mesopelagic zone. Such a biomass could play a substantial role in the biological carbon pump, and could potentially bolster future food security.

Uncertainty in mesopelagic fish biomass estimates could be reduced by (i) including more frequencies in the analysis to aid in determining size structure of resonant scatterers; (ii) development of an individual-based model to link DVM behaviour, weight/condition, swimbladder state, and volume to the environment, and (iii) obtaining more information on the size and depth distribution and density of siphonophores, both by collation of existing data and through the use of new technologies such as profiling acoustic optical systems (Marouchos *et al.*, 2016).

References

Aksnes, D. L., Røstad, A., Kaartvedt, S., Martinez, U., Duarte, C. M., and Irigoien, X. 2017. Light penetration structures the deep acoustic scattering layers in the global ocean. Science Advances, 3: 1–6.

Anderson, T. R., Martin, A. P., Lampitt, R. S., Trueman, C. N., Henson, S. A., and Mayor, D. J. 2018. Quantifying carbon fluxes from primary production to mesopelagic fish using a simple food web model. ICES Journal of Marine Science, doi: 10.1093/icesjms/fsx234.

Andreeva, I. B., Galybin, N. N., and Tarasov, L. L. 2000. Vertical structure of the acoustic characteristics of deep scattering layers in the ocean. Acoustical Physics, 46: 505–510.

Baik, K. 2013. Comment on 'Resonant acoustic scattering by swimbladder-bearing fish' [J. Acoust. Soc. Am. 64, 571–580 (1978)] (L). The Journal of the Acoustical Society of America, 133: 5–8.

Bardarson, B. 2013. Modelled Target Strengths of Three Lanternfish (Family: Myctophidae) in the North East Atlantic Based on Swimbladder and Body Morphology. University of St Andrews, Scotland. 97 pp.

Barham, E. G. 1963. Siphonophores and the deep scattering layer. Science, 140: 826–828.

Barham, E. G. 1966. Deep scattering layer migration and composition: observations from a diving saucer. Science, 151: 1399–1403.

Barham, E. G. 1971. Deep-sea fishes: lethargy and vertical orientation. *In* Proceedings of an international symposium on biological sound scattering in the ocean, pp. 100–118. Ed. by G. B. Farquhar. U.S. Government Printing Office, Washington, DC.

Bianchi, D., Galbraith, E. D., Carozza, D. A., Mislan, K. A. S., and Stock, C. A. 2013. Intensification of open-ocean oxygen depletion by vertically migrating animals. Nature Geoscience, 6: 545–548.

Bone, Q., Marshall, N. B., and Blaxter, J. H. S. 1995. Biology of Fishes. Blackie, New York.

Brierley, A. S. 2014. Diel vertical migration. Current Biology, 24: R1074–R1076.

Butler, J. L., and Pearcy, W. G. 1972. Swimbladder morphology and specific gravity of myctophids off oregon. Journal of the Fisheries Research Board of Canada, 29: 1145–1150.

Capen, R. L. 1967. Swimbladder Morphology of Some Mesopelagic Fishes in Relation to Sound Scattering. Research Report 1447. US Navy Electronics Laboratory, San Diego, California. 1–31 pp.

Chu, D. 2011. Technology evolution and advances in fisheries acoustics. Journal of Marine Science and Technology, 19: 245–252.

Chu, D., Foote, K. G., and Stanton, T. K. 1993. Further analysis of target strength measurements of Antarctic krill at 38 and 120 kHz: comparison with deformed cylinder model and inference of orientation distribution. The Journal of the Acoustical Society of America, 93: 2985–2988.

Clarke, M. R. 1996. The role of cephalopods in the world's oceans: general conclusion and the future. Philosophical Transactions of the Royal Society B: Biological Sciences, 351: 1105–1112.

Coetzee, J. 2000. Use of a shoal analysis and patch estimation system (SHAPES) to characterise sardine schools. Aquatic Living Resources, 13: 1–10.

Cox, M. J., Watkins, J. L., Reid, K., and Brierley, A. S. 2011. Spatial and temporal variability in the structure of aggregations of Antarctic krill (Euphausia superba) around South Georgia, 1997–1999. ICES Journal of Marine Science, 68: 489–498.

Davison, P. C. 2011a. The Export of Carbon Mediated by Mesopelagic Fishes in the Northeast Pacific Ocean. University of California, San Diego. 149 pp.

Davison, P. C. 2011b. The specific gravity of mesopelagic fish from the northeastern Pacific Ocean and its implications for acoustic backscatter. ICES Journal of Marine Science, 68: 2064–2074.

Davison, P. C., Checkley, D. M., Koslow, J. A., and Barlow, J. 2013. Carbon export mediated by mesopelagic fishes in the northeast Pacific Ocean. Progress in Oceanography, 116: 14–30.

Davison, P. C., Koslow, J. A., and Kloser, R. J. 2015. Acoustic biomass estimation of mesopelagic fish: backscattering from individuals, populations, and communities. ICES Journal of Marine Science, 72: 1413–1424.

Denton, E. J. 1961. The buoyancy of fish and cephalopods. Progress in Biophysics and Molecular Biology, 11: 177–234.

Flynn, A. J., and Kloser, R. J. 2012. Cross-basin heterogeneity in lanternfish (family Myctophidae) assemblages and isotopic niches (δ 13C and δ 15N) in the southern Tasman Sea abyssal basin. Deep-Sea Research Part I: Oceanographic Research Papers, 69: 113–127.

Flynn, A. J. and Pogonoski, J. J. 2012. Guide to Mesopelagic Fishes of the Southern Tasman Sea. CSIRO Marine and Atmospheric Research, Hobart, Australia. 221 pp.

Foote, K. G. 1980. Importance of the swimbladder in acoustic scattering by fish: a comparison of gadoid and mackerel target strengths. The Journal of the Acoustical Society of America, 67: 2084–2089.

Foote, K. G. 1987. Fish target strengths for use in echo integrator surveys. The Journal of the Acoustical Society of America, 82: 981–987.

Forland, T. N., Hobæk, H., and Korneliussen, R. J. 2014. Scattering properties of Atlantic mackerel over a wide frequency range. ICES Journal of Marine Science, 71: 1904–1912.

Fulton, E. A., Link, J. S., Kaplan, I. C., Savina-Rolland, M., Johnson, P., Ainsworth, C., Horne, P. et al. 2011. Lessons in modelling and management of marine ecosystems: the Atlantis experience. Fish and Fisheries, 12: 171–188.

Gascuel, D., Morissette, L., Palomares, M. L. D., and Christensen, V. 2008. Trophic flow kinetics in marine ecosystems: toward a theoretical approach to ecosystem functioning. Ecological Modelling, 217: 33–47.

Gee, J. H. 1983. Ecologic implications of buoyancy control in fish. *In* Fish Biomechanics, pp. 140–176. Ed. by P. W. Webb and D. Weihs. Praeger, New York.

Giering, S. L. C., Sanders, R., Lampitt, R. S., Anderson, T. R., Tamburini, C., Boutrif, M., Zubkov, M. V. et al. 2014. Reconciliation of the carbon budget in the ocean's twilight zone. Nature, 507: 480–483.

Gjøsaeter, J. and Kawaguchi, K. 1980. A review of the world resources of mesopelagic fish. FAO Fisheries Technical Paper, I–151.

Handegard, N. O., Buisson, L. D., Brehmer, P., Chalmers, S. J., De Robertis, A., Huse, G., Kloser, R. et al. 2013. Towards an acoustic-based coupled observation and modelling system for monitoring and predicting ecosystem dynamics of the open ocean. Fish and Fisheries, 14: 605–615.

Handegard, N. O., Demer, D. A., Kloser, R., Lehodey, P., Maury, O., and Simrad, Y. 2010. Toward a global ocean ecosystem mid-trophic automatic acoustic sampler (MAAS). *In* Proceedings of OceanObs'09: Sustained Ocean Observations and Information for Society 2. Ed. by J. Hall, D. E. Harrison, and D. Stammer. ESA Publication, Venice.

Haraldsson, M., Tönnesson, K., Tiselius, P., Thingstad, T. F., and Aksnes, D. L. 2012. Relationship between fish and jellyfish as a function of eutrophication and water clarity. Marine Ecology Progress Series, 471: 73–85.

Hersey, J., Backus, R., and Hellwig, J. 1962. Sound-scattering spectra of deep scattering layers in the western North Atlantic Ocean. Deep Sea Research Part I: Oceanographic Research Papers, 8: 196–210.

Heymans, J. J., Coll, M., Libralato, S., Morissette, L., and Christensen, V. 2014. Global patterns in ecological indicators of marine food webs: a modelling approach. PLoS One, 9: e95845.

Holliday, D. V. 1972. Resonance structure in echoes from schooled pelagic fish. The Journal of the Acoustical Society of America, 51: 1322.

Holliday, D. V., Pieper, R. E., and Kleppel, G. S. 1989. Determination of zooplankton size and distribution with multifrequency acoustic technology. ICES Journal of Marine Science, 46: 52–61.

Irigoien, X., Klevjer, T. A., Røstad, A., Martinez, U., Boyra, G., Acuña, J. L., Bode, A. et al. 2014. Large mesopelagic fishes biomass and trophic efficiency in the open ocean. Nature Communications, 5: 3271.

Jansen, M. J. W. 1999. Analysis of variance designs for model output. Computer Physics Communications, 117: 35–43.

Jennings, S., and Collingridge, K. 2015. Predicting consumer biomass, size-structure, production, catch potential, responses to fishing and associated uncertainties in the world's marine ecosystems. PLoS One, 10: 1–28.

Kaartvedt, S., Staby, A., and Aksnes, D. L. 2012. Efficient trawl avoidance by mesopelagic fishes causes large underestimation of their biomass. Marine Ecology Progress Series, 456: 1–6.

Kalish, J. M., Greenlaw, C. F., Pearcy, W. G., and Holliday, D. V. 1986. The biological and acoustical structure of sound scattering layers off oregon. Deep Sea Research Part A, Oceanographic Research Papers, 33: 631–653.

Klevjer, T. A., Irigoien, X., Røstad, A., Fraile-Nuez, E., Benítez-Barrios, V. M., and Kaartvedt, S. 2016. Large scale patterns in vertical distribution and behaviour of mesopelagic scattering layers. Scientific Reports, 6: 19873.

Kloser, R. J., Ryan, T., Sakov, P., Williams, A., and Koslow, J. A. 2002. Species identification in deep water using multiple acoustic frequencies. Canadian Journal of Fisheries and Aquatic Sciences, 59: 1065–1077.

Kloser, R. J., Ryan, T. E., Keith, G., and Gershwin, L. 2016. Deep-scattering layer, gas-bladder density, and size estimates using a two-frequency acoustic and optical probe. ICES Journal of Marine Science, 73: 2037–2048.

Kloser, R. J., Ryan, T. E., Young, J. W., and Lewis, M. E. 2009. Acoustic observations of micronekton fish on the scale of an ocean basin: potential and challenges. ICES Journal of Marine Science, 66: 998–1006.

Koslow, J. A., Kloser, R. J., and Williams, A. 1997. Pelagic biomass and community structure over the mid-continental slope off southeastern Australia based upon acoustic and midwater trawl sampling. Marine Ecology Progress Series, 146: 21–35.

Lavery, A. C., Chu, D., and Moum, J. N. 2010. Measurements of acoustic scattering from zooplankton and oceanic microstructure using a broadband echosounder. ICES Journal of Marine Science, 67: 379–394.

Lavery, A. C., Wiebe, P. H., Stanton, T. K., Lawson, G. L., Benfield, M. C., and Copley, N. 2007. Determining dominant scatterers of sound in mixed zooplankton populations. The Journal of the Acoustical Society of America, 122: 3304–3326.

Lehodey, P., Conchon, A., Senina, I., Domokos, R., Calmettes, B., Jouanno, J., Hernandez, O. et al. 2014. Optimization of a micronekton model with acoustic data. ICES Journal of Marine Science, 72: 1399–1412.

Lehodey, P., Senina, I., and Murtugudde, R. 2008. A spatial ecosystem and populations dynamics model (SEAPODYM) – modeling of tuna and tuna-like populations. Progress in Oceanography, 78: 304–318.

Love, R. H. 1978. Resonant acoustic scattering by swimbladder-bearing fish. The Journal of the Acoustical Society of America, 64: 571.

Love, R. H., Fisher, R. A., Wilson, M. A., and Nero, R. W. 2004. Unusual swimbladder behavior of fish in the Cariaco Trench. Deep Sea Research Part I: Oceanographic Research Papers, 51: 1–16.

Love, R. H., Thompson, C. H., and Nero, R. W. 2003. Changes in volume reverberation from deep to shallow water in the eastern Gulf of Mexico. The Journal of the Acoustical Society of America, 114: 2698.

Mackie, G. O., Pugh, P. R., and Purcell, J. E. 1988. Siphonophore Biology. Advances in Marine Biology, 24: 97–262.

Maclennan, D. N., Fernandes, P. G., and Dalen, J. 2002. A consistent approach to definitions and symbols in fisheries acoustics. ICES Journal of Marine Science, 59: 365–369.

Marouchos, A., Sherlock, M., Kloser, R. J., Ryan, T., and Cordell, J. 2016. A profiling acoustic and optical system (pAOS) for pelagic studies; Prototype development and testing. In OCEANS 2016 - Shanghai. IEEE. pp. 1–6.

Marshall, N. 1971. Swimbladder development and the life of deep sea fishes. In Proceedings of an International Symposium on Biological Sound Scattering in the Ocean, pp. 69–73. Ed. by G. B. Farquhar. Department of the Navy, Washington, DC.

Moser, H. G. (Ed). 1996. The Early Stages of Fishes in the California Current Region. Allen press, Lawrence, Kansas.

Murphy, E. J., Watkins, J. L., Trathan, P. N., Reid, K., Meredith, M. P., Thorpe, S. E., Johnston, N. M. et al. 2007. Spatial and temporal operation of the Scotia Sea ecosystem: a review of large-scale links in a krill centred food web. Philosophical Transactions of the Royal Society of London. Series B, Biological Sciences, 362: 113–148.

Musayeva, E. 1976. Distribution of siphonophores in the eastern part of the Indian Ocean. Trudy Institufa Oceanologii, 105: 171–197.

Neighbors, M. A., and Nafpaktitis, B. G. 1982. Lipid compositions, water contents, swimbladder morphologies and buoyancies of nineteen species of midwater fishes (18 myctophids and 1 neoscopelid). Marine Biology, 66: 207–215.

Netburn, A. N., and Koslow, J. A. 2015. Dissolved oxygen as a constraint on daytime deep scattering layer depth in the southern California current ecosystem. Deep-Sea Research Part I: Oceanographic Research Papers, 104: 149–158.

Pakhomov, E. A. and Yamamura, O. 2010. Report of the Advisory Panel on Micronekton Sampling Inter-calibration Experiment. PICES Scientific Report, No 38. pp 108.

Pauly, D., Graham, W., Libralato, S., Morissette, L., and Deng Palomares, M. L. 2009. Jellyfish in ecosystems, online databases, and ecosystem models. Hydrobiologia, 616: 67–85.

Pickwell, G. V. 1966. Physiological dynamics of siphonophores from deep scattering layers: size of gas-filled floats and rate of gas production. U.S. Navy Electronics Laboratory, San Diego, California. 50 pp.

Proud, R. 2016. A Biogeography of the Mesopelagic Community. University of St Andrews, Scotland.

Proud, R., Cox, M. J., and Brierley, A. S. 2017. Biogeography of the global ocean's mesopelagic zone. Current Biology, 27: 113–119.

Proud, R., Cox, M. J., Wotherspoon, S., and Brierley, A. S. 2015. A method for identifying sound scattering layers and extracting key characteristics. Methods in Ecology and Evolution, 6: 1190–1198.

Roberts, C. M., O'Leary, B. C, McCauley, D. J., Cury, P. M., Duarte, C. M., Lubchenco, J., Pauly, D. et al. 2017. Marine reserves can mitigate and promote adaptation to climate change. Proceedings of the National Academy of Sciences, 114: 6167–6175.

Robison, B. H., Reisenbichler, K. R., Sherlock, R. E., Silguero, J. M. B., and Chavez, F. P. 1998. Seasonal abundance of the siphonophore, Nanomia bijuga, in Monterey Bay. Deep-Sea Research Part II: Topical Studies in Oceanography, 45: 1741–1751.

Rogers, C. 1978. Aggregation of the siphonophore Nanomia cara in the Gulf of Maine: observations from a submersible. Fishery Bulletin, 76: 281–284.

Rosenberg, A. A., Fogarty, M. J., Cooper, A. B., Dickey-Collas, M., Fulton, E. A., Gutierrez, N. L., Hyde, K. J. W. et al. 2014. Developing new approaches to global stock status assessment and fishery production potential of the seas. FAO Fisheries and Aquaculture Circular No. 1086. FAO, Rome. 175 pp.

Saltelli, A., Annoni, P., Azzini, I., Campolongo, F., Ratto, M., and Tarantola, S. 2010. Variance based sensitivity analysis of model output. Design and estimator for the total sensitivity index. Computer Physics Communications, 181: 259–270.

Schlining, B., and Stout, N. 2006. MBARI's video annotation and reference system. In OCEANS 2006, pp. 1–5. IEEE.

Scott, F., Blanchard, J. L., and Andersen, K. H. 2014. mizer: an R package for multispecies, trait-based and community size spectrum ecological modelling. Methods in Ecology and Evolution, 5: 1121–1125.

Scoulding, B., Chu, D., Ona, E., and Fernandes, P. G. 2015. Target strengths of two abundant mesopelagic fish species. The Journal of the Acoustical Society of America, 137: 989–1000.

Simmonds, E. J., and MacLennan, D. N. 2005. Fisheries Acoustics: Theory and Practice. 2nd edn. Blackwell Science, Oxford. 437 pp.

Sobol, I. 1967. On the distribution of points in a cube and the approximate evaluation of integrals. USSR Computational Mathematics and Mathematical Physics, 7: 86–112.

St John, M. A., Borja, A., Chust, G., Heath, M., Grigorov, I., Mariani, P., Martin, A. P. et al. 2016. A dark hole in our understanding of marine ecosystems and their services: perspectives from the mesopelagic community. Frontiers in Marine Science, 3: 1–6.

Stanton, T. K. 1988. Sound scattering by cylinders of finite length. II. Elastic cylinders. The Journal of the Acoustical Society of America, 83: 64–67.

Strasberg, M. 1953. The pulsation frequency of nonspherical gas bubbles in liquids. The Journal of the Acoustical Society of America, 25: 536.

Thompson, C. H., and Love, R. H. 1996. Determination of fish size distributions and areal densities using broadband low-frequency measurements. ICES Journal of Marine Science, 53: 197–201.

Trebilco, R., Baum, J. K., Salomon, A. K., and Dulvy, N. K. 2013. Ecosystem ecology: size-based constraints on the pyramids of life. Trends in Ecology and Evolution, 28: 423–431.

Warren, J. 2001. In situ measurements of acoustic target strengths of gas-bearing siphonophores. ICES Journal of Marine Science, 58: 740–749.

Weston, D. 1967. Sound Propagation in the Presence of Bladder Fish, in Underwater Acoustics. Plenum, New York. 55–58 pp.

Yasuma, H., Sawada, K., Takao, Y., Miyashita, K., and Aoki, I. 2010. Swimbladder condition and target strength of myctophid fish in the temperate zone of the Northwest Pacific. ICES Journal of Marine Science, 67: 135–144.

Yasuma, H., and Yamamura, O. 2010. Comparison between acoustic estimates. *In* Report of the Advisory Panel on Micronekton Sampling Inter-Calibration Experiment, pp. 51–57. Ed. by E. Pakhomov and O. Yamamura. North Pacific Marine Science Organization (PICES), Sydney.

Ye, Z. 1998. Low-frequency acoustic scattering by gas-filled prolate spheroids in liquids. II. Comparison with the exact solution. The Journal of the Acoustical Society of America, 103: 822.

Handling editor: David Demer